

# **Blast Barrier Effectiveness Simulations**

by

Tommy L. Bevins<sup>1</sup>, James T. Baylot<sup>1</sup>, David L. Littlefield<sup>2</sup>  
<sup>1</sup>U.S. Army Engineer Research and Development Center (ERDC)  
Vicksburg, MS

<sup>2</sup> Texas Institute for Computational and Applied Mathematics (TICAM), University of Texas,  
Austin, TX

## **Abstract**

Blast barrier walls are placed around a building to provide protection to that building from the effects of an explosive attack by terrorists. The ERDC is involved in an experimental program designed to study the effectiveness of those barrier walls for a range of charge weights, charge standoffs and wall heights. These experiments provide excellent data on the effectiveness of the walls for a range of conditions, but understanding the phenomenology is limited using only the experimental data. Under High-Performance-Computing (HPC) Modernization Office (HPCMO) Challenge Project C-22 “Development of Standards for Stand-Off Distances and Blast Walls for Force Protection,” HPC simulations of these experiments were performed to assist in understanding this complex phenomenology. In this paper, analytical and experimental results are compared. Visualizations from the analyses are used to understand the complex flow of the airblast around the barrier wall. Recent improvements to the software used to perform the simulations are also discussed.

## **Background**

The ERDC, Geotechnical and Structures Laboratory, is the lead laboratory for research in the Civil Engineering area of survivability and protective structures (S&PS) under the Tri-Service Project Reliance Civil Engineering Science and Technology Plan. The S&PS research program is focused on the warfighter’s needs for force protection and counter-terrorist threats. One of the most important objectives of this research is to provide engineering tools to allow rapid evaluation of the effectiveness of counter-terrorism technology. Blast barriers are used to reduce blast loads on protected structures. The ERDC has conducted a series of small-scale blast-barrier experiments (Figure 1). Two control experiments were conducted without a barrier wall to provide a comparison with those cases where the wall was present. In the experiments including the walls, four different charge masses, three standoff distance and five wall heights were used. In each of these experiments, airblast pressure measurements were made at the locations shown in Figure 1.

---

Distribution is authorized to U.S. Government agencies and their contractors; critical technology, June 2001. Other requests for this document shall be referred to U.S. Army Engineer Research and Development Center, 3909 Halls Ferry Rd., Vicksburg, MS 39180-6199.

Comparisons of blast wall experiments to free-field experiments demonstrate that the blast wall is very effective in reducing the impulse at points very near to the back of the blast wall, but the effectiveness of the wall decreases with increasing distance from the wall. The effect of the blast wall also decreases with increasing angle. For example, the impulses from the gages very close to the wall along the zero-degree azimuth (see Figure 1) are significantly lower than the associated free-field impulse, but the gages close to the wall along the 83-degree azimuth are not significantly lower than free-field. These experiments provide an excellent means of validating numerical simulations of blast over barrier walls. The validated simulations are used to assist in understanding the phenomenology and to develop blast-barrier design software.

### **Analysis Methodology and Code Scalability**

The analysis approach was to use the HPCMO Common HPC Software Support Initiative (CHSSI) computational structural mechanics scalable software, CTH, to predict the airblast environment. The CTH software is a multi-dimensional, multi-material, finite-volume shock physics code that models shocks and the multiphase behavior of materials. The mass, momentum, and energy conservation equations are integrated explicitly in time using a two-step Eulerian scheme. First, a Lagrangian step, in which the computational cells are allowed to distort, is performed. Then in the second step, the distorted cells are mapped back onto the Eulerian mesh. The analysis domain is divided such that approximately the same number of analysis cells is mapped on to each processor. Analyses were performed on both the IBM SP and the CRAY T3E available at the ERDC Major Shared Resource Center (MSRC).

The analyses of each of these sets of experiments required modelling a significant volume around the structure and the explosives. Relatively fine cell spacing is required to capture the rise times associated with a structure placed close to the explosives. These small cell sizes require small time steps to numerically integrate the equations of motion of the systems involved. A large number of cells were evaluated over a large number of time steps. Thus, scalability of the software is critical.

Scalability for CTH has been evaluated for four of the HPC systems (see Table 1) at the ERDC MSRC. A baseline analysis consisting of 400,000 cells was performed on a single processor of each of these systems. The number of cells analyzed was increased in proportion to the number of processors so that the number of cells on a single processor remained constant. The same number of cycles was performed for each analysis. For perfect scalability, the wall time would be constant as the number of processors and cells are increased. Wall times are plotted against the number of processors in Figure 2. As seen in this figure, for small numbers of processors, performance is best for the Pandion system. When the number of processors reaches 64, performance of the T3E is comparable to the Pandion, and T3E scalability is good up to 512 processors. At 512 processors, the wall time for the T3E is about 50-percent higher than for a single processor; thus, problem size can be increased by a factor of 512, while wall time only increases by 50 percent. Similar results are obtained for the Pandion at 100 processors. The problem size was increased by a factor of 100, with only a 57-percent increase in wall time. Scalability for the other two systems is also good.

Even with highly scalable software and the availability of large amounts of HPC compute time available under the challenge project, it is important to optimize the solution of the problem. The largest cell size that produces acceptable solutions should be used. A cell size study was performed using a one-dimensional-spherical (1-D) model. An initial analysis was performed using constant cell spacing equal to the explosive charge radius of 2.8 cm, Case F in Figures 3 and 4. A second run was then performed using smaller cell spacing. Progressively smaller cells were used. The cell size study was stopped when further refinement no longer caused an appreciable change in peak pressure or impulse over the range of standoff distances of interest in this problem. The minimum cell spacing was 0.07 cm in Case A. The peak pressure and impulse based on the smallest cell size analyzed were used as the converged solution in order to compute the percent error of the solutions for the other cell spacings. Percent error in pressure and impulse are plotted as a function of standoff in Figures 3 and 4, respectively. The criteria selected for optimum cell spacing was that the error in peak pressure not exceed 10 percent and that the error in impulse not exceed 5 percent over the range of charge standoffs considered. The desired level of accuracy can be obtained using a constant cell spacing of 0.3 cm near the charge. In this problem smaller cell sizes are needed near the charge. The cell sizes may be increased with distance from the charge. Another 1-D analysis was performed with a cell spacing of 0.3 cm near the charge and uniformly expanding the cell spacing to 2 cm at a standoff of 350 cm. The error in peak pressure and impulse for this mesh, Case K, is compared with the other 1-D simulations in Figures 3 and 4, respectively. The 1-D mesh sizing results were verified by performing two-dimensional (2-D), and three-dimensional (3-D) simulations using the cell spacings determined in the 1-D simulations. The 1-, 2-, and 3-D pressures and impulses for a station 25 at a range of 100 cm are compared in Figures 5 and 6, respectively. These studies also provide an indication of the numerical accuracy of the solutions obtained for the full model.

### **Comparison with Experimental Results**

The cell spacings determined above were used to model one of the control experiments. The explosive charge was placed on a reflective boundary that represented the steel plate used in the experiment. Two control experiment results and predicted blast pressure histories are compared in Figure 7 for a gage at a range of 50 cm. These comparisons indicated that the model gave a reasonable prediction of pressure and impulse. The computed peak pressure is ten percent low and the time of arrival (toa) is delayed. These characteristics in the primary shock plus similar characteristics in the secondary shock indicates the modeled explosive is slightly undersized.

Several modifications were needed to simulate the experiments that included the blast wall. In order to effectively model the thickness of the model blast barrier, the minimum cell spacing had to be decreased from 0.3 to 0.2 cm. This spacing was held constant up to and through the barrier wall. The critical time step for the explicit integration of the problem is a function of the cell spacing divided by the wave speed in the material. The 0.2 cm cells in the steel wall control the time step for the solution of the barrier wall experiments, and thus control the number of cycles needed to complete the solution. This significantly affects the amount of time required to complete the solution.

In the initial analyses, the barrier wall was placed directly on top of the reflecting boundary representing the steel bottom plate. There is, however, no method available in CTH for attaching the blast barrier wall to the reflective boundary. In the experiment, the wall behaved as a rigid wall. In the analysis, significant deformation occurred in the wall. That error was overcome by modeling the bottom plate as steel and attaching the barrier wall to it. The final model is shown as Figure 8. This modeling technique corrected the problem of excessive wall deformations, but created another problem. The new model had the explosive charge placed directly on the bottom plate. Modeling the severe damage to the bottom plate significantly increased run time.

Computed peak pressures along the zero degree and 83 degree line of gages are compared to experimental data in Figure 9. This shows that the magnitude of the pressure is approximately correct and that the correct trends in pressure with range are matched. Similarly, impulse histories along the zero degree and 83 degree line of gages are compared in Figure 10. Again the magnitudes and trends of the impulses match those of the experiments. These comparisons indicate the analysis results may be confidently used to try to understand the phenomenology of the experiments.

### **Improvements to CTH**

Enhancements to the CTH code made by TICAM under the ERDC MSRC Programming Environment and Training Program have significantly improved the effectiveness of performing these types of simulations. The automatic mesh refinement (AMR) (Littlefield, et al, 2000) capability refines the model when and where small cell sizes are needed. Thus, the analyst can start with large cell sizes and the code will refine them only where needed to provide an accurate solution. It will then coarsen the model when the finer cells are no longer needed. This should significantly reduce the number of active cells, could increase the required time step and should cause a major reduction in run times without sacrificing solution accuracy.

A rigid obstacle model added to CTH by TICAM (Littlefield, 2001) alleviates some problems encountered in performing these simulations. Wall deformations were negligible in the experiments. The bottom plate of the experiment can be changed back to a rigid boundary, because the blast wall can now be replaced with a rigid obstacle. This relieves the problems caused by the detonation of the explosives in contact with the steel. Since the steel wall no longer has to be modeled, the minimum cell size may be increased from 0.2 to 0.3 cm and the minimum time step is no longer computed based on the steel wall.

### **Evaluations of Improvements**

Initial test runs using AMR CTH demonstrate improvements over the serial and scalable non-AMR versions. A serial analysis used 2040 seconds to analyze a spherical blast. The AMR analysis required 626 seconds on one processor and 225 seconds running on 8 processors. Running the non-AMR test deck on 8 processors required 340 seconds. On this problem, the scalable AMR version is running 33 percent faster than the equivalent non-AMR analysis running on eight processors.

Rigid inclusions are providing additional improvements to the analysis stability and runtime. An analysis of a reduced size (3.8 million cells) blast wall problem computed 1233 cycles and simulated 0.3 ms of simulation time using steel to model the wall. A similar analysis, using rigid inclusions, computed 1259 cycles and complete 0.5ms simulation time in ten hours of wall time. The rigid inclusions showed a 67% increase in simulation time for the same amount of wall time. The analysis used 8 processors.

## **Conclusions**

The analyses performed using the original version of CTH under this challenge project have demonstrated that CTH reproduces experimental results for blast wall experiments. These analytical results have been used to understand the phenomenology associated with blast near walls. These analyses could not have been accomplished using this version of CTH without the extensive high-priority HPC resources provided under the challenge project.

The enhancements that have been made to CTH under the ERDC PET program have made it possible to analyze much more complicated problems in the future. Using the AMR and rigid obstacle models now available in CTH it will be possible to model a significant portion of a city to assist in understanding how the blast on one building is affected by the presence of other buildings. Future HPC challenge project time will allow ERDC researchers to develop a much needed model for quickly predicting blast loads in urban terrain.

## **Acknowledgments**

This research was conducted under the Army Force Protection from Terrorist Threats Research Development Test and Evaluation Program. The authors gratefully acknowledge permission from the Chief of Engineers to publish this paper.

## **References**

Littlefield, D.L., Oden, J.T., and Carey, G.F., 2000, "Adaptive mesh refinement in CTH: Implementations of block-adaptive multi-material refinement and advection algorithms," proceedings of HPC User's Group Conference, held June 5-8, 2000, Albuquerque, NM, [http://www.hpcmo.hpc.mil/Htdocs/UGC/UGC00/paper/david\\_littlefield\\_paper.pdf](http://www.hpcmo.hpc.mil/Htdocs/UGC/UGC00/paper/david_littlefield_paper.pdf)

Littlefield, D.L., 2001, "A brief description of new algorithms incorporated into CTH: a model for rigid obstacles and an interface for coupling with DYNA," to be presented and published at HPC User's Group Conference, Biloxi, MS, 18-21 June, 2001.

McGlaun, J.M., Thompson, S.L., and Elrick, M.G., 1990, "CTH: A Three-Dimensional Shock Wave Physics Code," *International Journal of Impact Engineering*, Vol 99, pp 351-360.

Table 1. System parameters for scalability study

	T3E	Osprey (IBM SP)	Pandion (IBM SP)	Origin
Processor type	Alpha	P2SC	POWER2	R10000
Number of processors	544	255	126	112
Processor speed	600 MHz	135 MHz	160 MHz	195 MHz
Total Gflops	634	137.7	80.6	49.9

Figure Captions

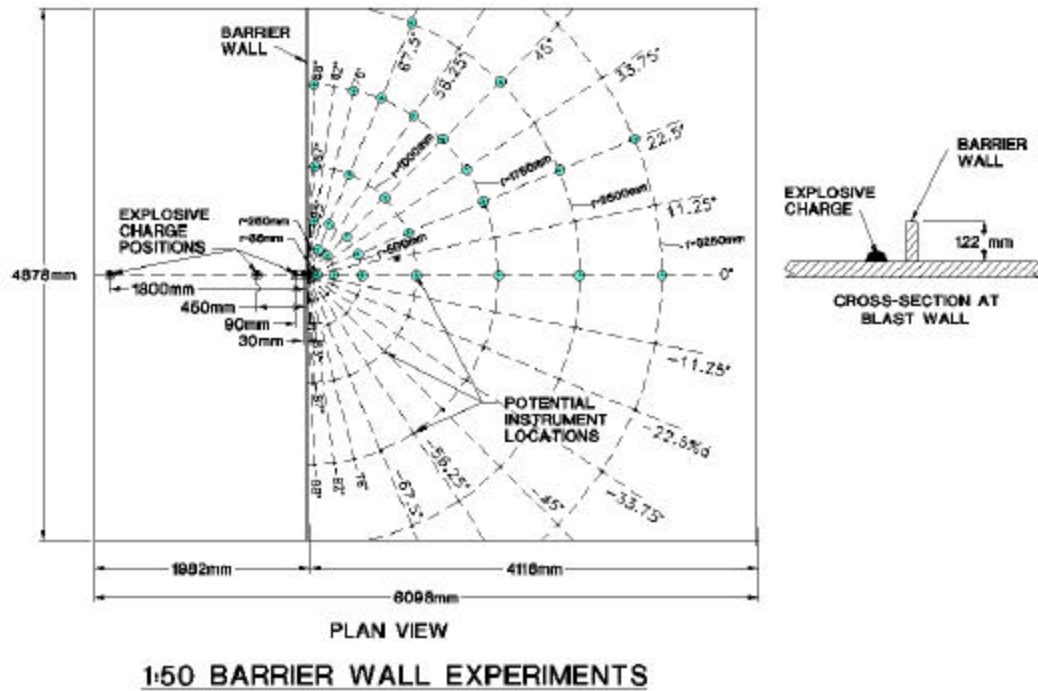


Figure 1 Blast Wall Experiment Layout

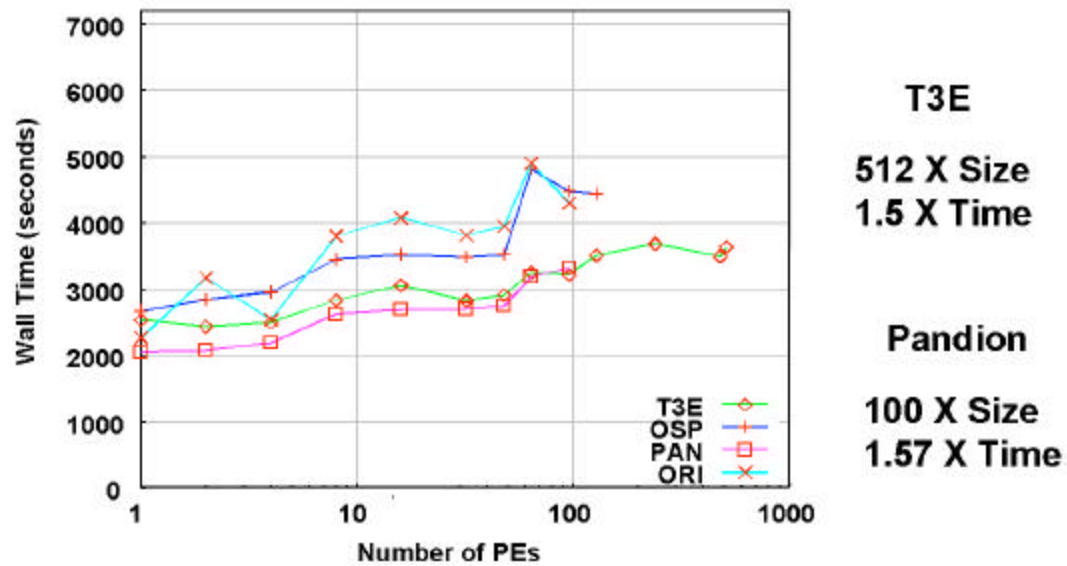


Figure 2 CTH Scalability

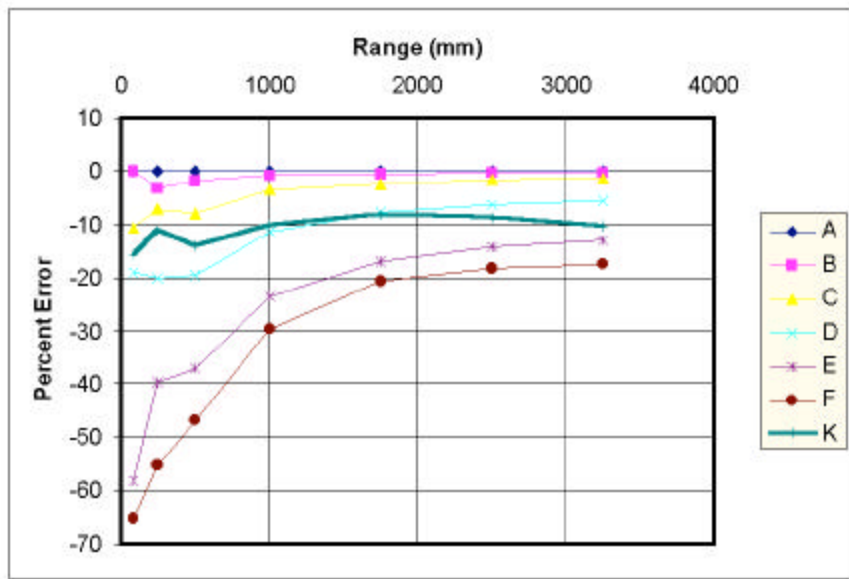


Figure 3 Peak Pressure Error, 1-D Simulations

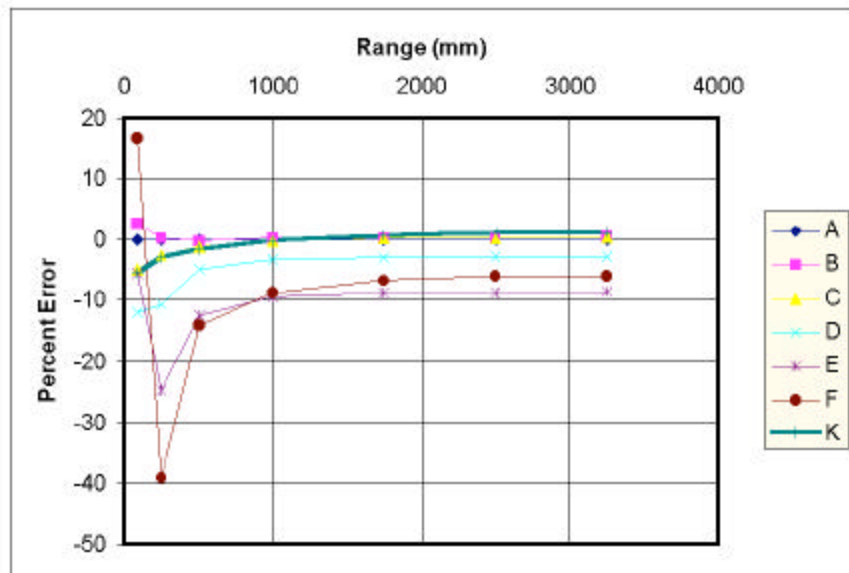


Figure 4 Impulse Error, 1-D Simulations



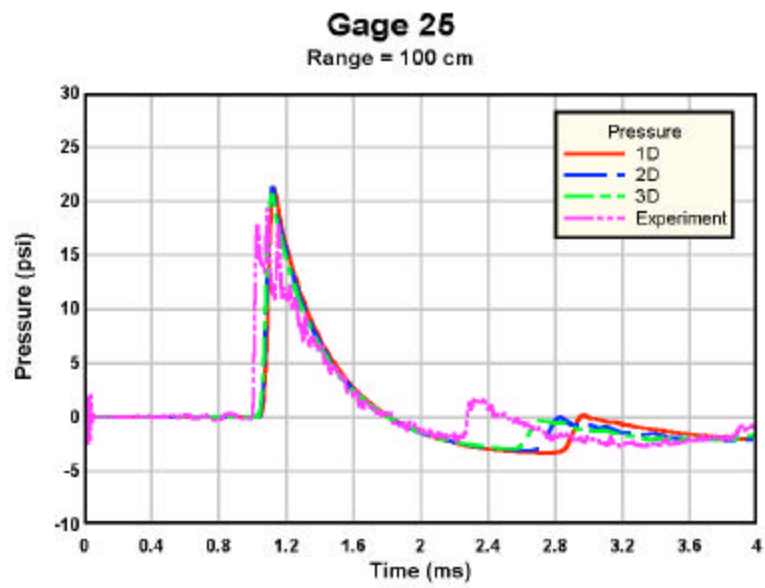


Figure 5 Pressure, 1-D, 2-D, 3D Verification

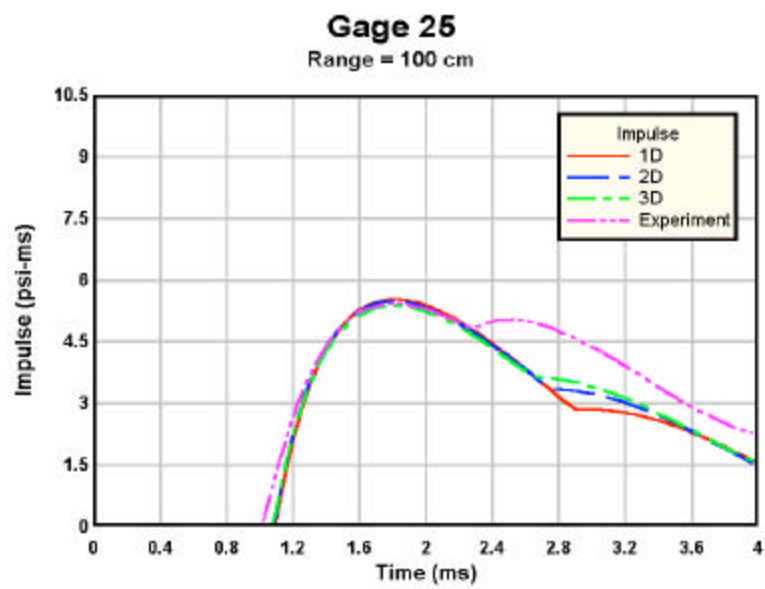


Figure 6 Impulse, 1-D, 2-D, 3-D Verification

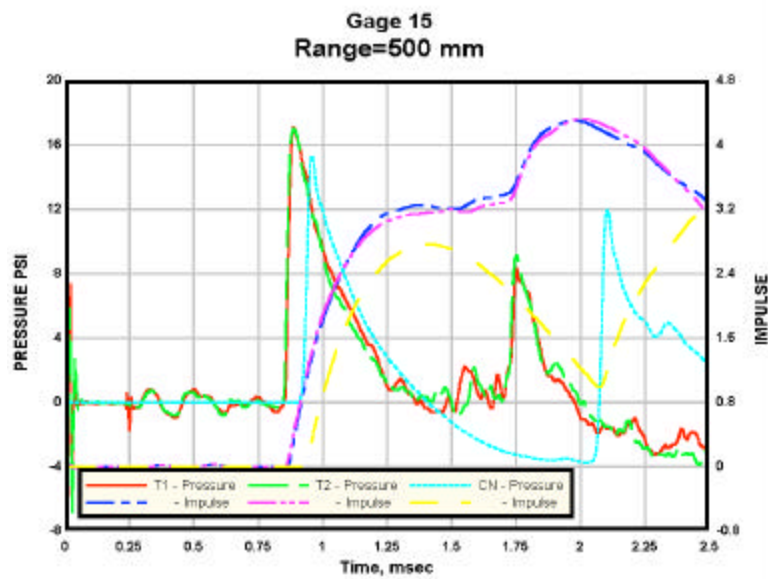


Figure 7 Pressure and Impulse Comparisons

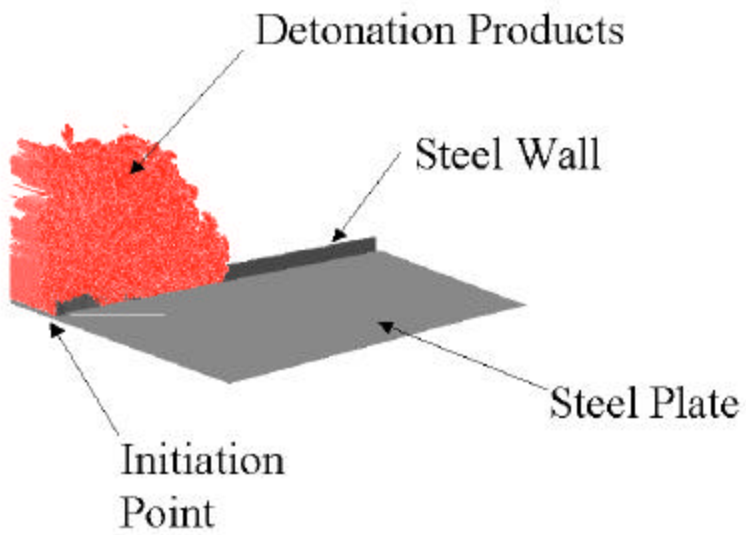


Figure 8 Model for Blast Wall Experiments

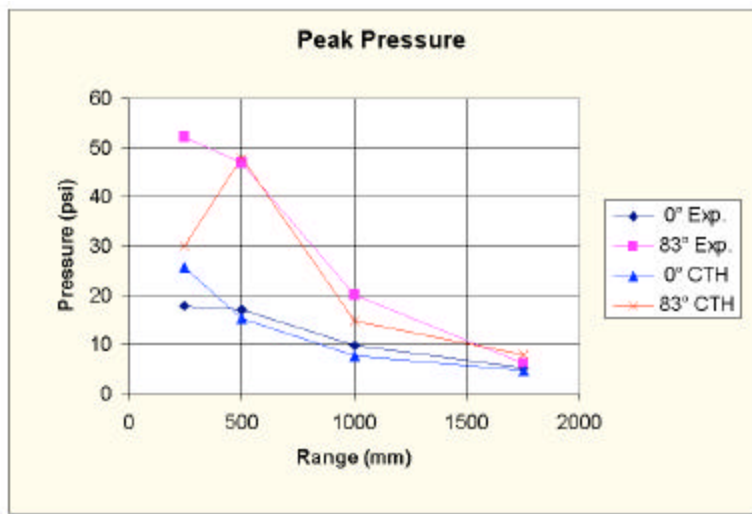


Figure 9 Peak Pressure Comparisons

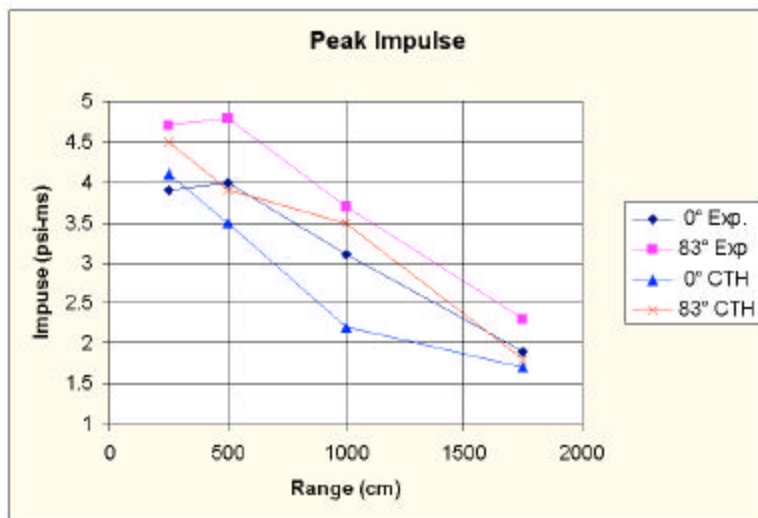


Figure 10 Peak Impulse Comparisons